Fuel 280 (2020) 118573

Contents lists available at ScienceDirect

Fuel

journal homepage: www.elsevier.com/locate/fuel

Full Length Article

Prediction of biogas production from chemically treated co-digested agricultural waste using artificial neural network

Fares Almomani

College of Engineering, Department of Chemical Engineering, Qatar University, P. O. Box 2713, Doha, Qatar

GRAPHICAL ABSTRACT

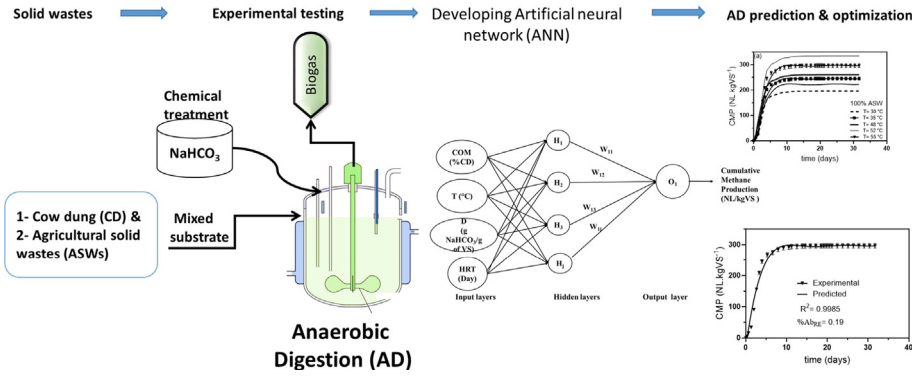

ARTICLE INFO

Keywords:
Co-digestion
Kinetic model
Lignin degradation
Biofuel potential
Agricultural biomass

ABSTRACT

The present study evaluates the effect of co-digestion of agricultural solid wastes (ASWs), cow manure (CM), and the application of chemical pre-treatment with $NaHCO_3$ on the performance of anaerobic digestion (AD) process. An Artificial neural network (ANN) algorithm was developed to model and optimize the cumulative methane production (CMP) from ASWs, CM, and their mixture under mesophilic and thermophilic conditions. The results demonstrated that co-digestion of ASWs with CM with a ratio of 70% to 30% produced the highest CMP of 334 ± 4 NL/kgVS in comparison with 230 ± 10 NL/kgVS for mono-digested substrate. The CMP was the highest for the substrate with moisture content (%MC) in the range of 34% to 48%, and it decreased for % MC > 50%. The chemical treatment with $NaHCO_3$ improved the biodegradability of the substrate and increased the CMP by at least 43% with reference to the untreated substrate. An ANN model consists of three layers, 15 neutrons and 260 *epochs* accurately predict the CMP with 99.1% of data within ± 10% deviation of the mean experimental value. The developed model can be used to forecast the CMP as a function of operating temperature, the substrate composition, and chemical dose, and can be used for scaling-up and cost analysis purposes.

1. Introduction

The high demand for the use of fossil fuels has resulted in a rise in global pollution and carbon emissions at an alarming level bringing worldwide attention to the importance of renewable energy resources [1–4]. Additionally, agricultural activities produce large quantities of agricultural solid wastes (ASWs) that requires proper management and disposal. The most commonly used practice to reduce the accumulation

E-mail address: falmomani@qu.edu.qa.

https://doi.org/10.1016/j.fuel.2020.118573
Received 5 April 2020; Received in revised form 1 June 2020; Accepted 29 June 2020
Available online 17 July 2020

of ASWs is incineration. However, burning ASWs releases greenhouse gases (GHG) and fine particles to the atmosphere and contributes to air pollution and increased global warming [5,6]. Agriculture solid waste also includes a huge amount of manure produced from animal meat and dairy production farms [7]. It was reported that average-sized dairy cow produce up 22 Mg/yr of manure with an equivalent of 2.5 Mg/yr and 2.3 Mg/yr of chemical oxygen demand (COD) and volatile solids (VS), which need urgent treatment or suitable disposal strategies [8–10].

Anaerobic digestion (AD) is a verified treatment technology and well-established engineering concept that can be employed to treat ASWs and manure, decrease the emission of GHG and produce biofuel [11]. Co-anaerobic digestion (Co-AD) of ASWs with animal manure is a promising management methodology with advantages of easy operation, sustainability, and high energy output for the production of biogas and fertilizers [12–14]. Mono-AD and Co-AD processes were utilized for the treatment of different substrates. Co-AD resolves technical problems, including carbon to nitrogen ratio (C:N) limitations, substrate biodegradability (Bio_{sub}), pH, inhibition, and moisture content (%MC), thus, has shown a high reaction rate, a high biofuel production, and increased performance over mono-AD [15–19].

Agricultural solid wastes (ASWs) contain, in general, materials that can be classified as cellulose (Ce), hemicellulose (HCe), and lignin (Li). Ce and HCe are biodegradable compounds and can be easily digested in AD process. However, lignin (Li) based materials are nonbiodegradable and a pre-treatment process is required to facilitate their digestion [20]. Mechanical and thermal pre-treatment were used to improve the digestion of Li by reducing the particle size, increasing the surface area, and breaking down Li to simpler compounds. Biological pre-treatment using microorganisms was also used to enhance AD of Li. Lalak et al. [21] showed that *F. velutipes* microorganisms improved the biodegradation of Li while increasing the biogas production by 20% compared to the untreated substrate. However, the high cost and difficult control requirements associated with these processes (mechanical, thermal, and biological) limit their applications. Chemical treatment using acidic, basic, and oxidizing agents has demonstrated good results for increasing dissolved solids (DSs), increasing the internal surface area of the substrate, break down the structure of Li, reduce the degree of inhibition, and advance the efficiency of AD [20,22–27]. The added chemicals create alkalinity (ALK) inside the anaerobic digester and supports the control of the pH. As such, basic treatment with a chemical such as sodium bicarbonate ($NaHCO_3$) provides effective Li pre-treatment and increases the performance of AD [28].

Different parameters including the operating temperature (T_{op}), chemical pre-treatment, substrate composition (COM_{sub}), %MC, total solids (TS), VS, Bio_{sub}, C:N ratio and hydraulic retention time (HRT) can be manipulated to enhance the performance of AD process. While thermophilic (50–60 °C) AD process is particularly beneficial for biogas production, digesters operated under mesophilic conditions (30 – 45 °C) are more common due to simple process control, improved sludge dewatering properties, and low-heating requirements[29,30]. Sambo et al. [31] showed that Co-AD of cow manure-water mixture at 50 °C generated the optimum biogas yield followed by 60 and 40 °C. Mahanta et al. [32] attained the maximum biogas production from cattle manure-water mixture at 35 °C followed by 45, 30, and 40 °C. Other research has tested the biogas production at differing T_{op} from different substrates [8,9]. However, a well-established rule concerning the effect of T_{op} on the performance of the AD process in both mesophilic and thermophilic conditions has not been reported. The literature review revealed high discrepancies about the influence of chemical pre-treatment, COM_{sub}, %MC, TS, VS, Bio_{sub}, C:N ratio and HRT on the performance of AD process which should be considered before employing AD at a large scale [33–37].

The kinetic of the AD is another important factor to consider for scale-up purposes. Ultimate methane (CH_4) yield, cone and modified Gompertz models have been used to determine the kinetic parameters and calculate cumulative methane production (CMP) by the AD [38–40]. However, these models can be only used with available experimental data under predetermined conditions, and cannot be used to predict process performance under unexamined operational conditions. As the AD is a highly non-linear and complex process and the generation of experimental data requires large volumes of substrates and takes a long time, experiment data for a wide range of operating conditions are limited and the available data are not enough to carry out accurate design and/or process optimization. Therefore, there is an urgent need to develop a systematic approach to model, optimize, predict, and control the performance of the AD process under a wide range of conditions.

Recently, the use of artificial intelligence (AI) methods, including artificial neural networks (ANN) have been successful in predicting the kinetic behavior of different engineering processes. ANNs were suggested to be the most suitable algorithm to predict the behavior of different linear and non-linear processes with a high amount of accuracy. Generally, the prediction accuracy is dependent upon the input data points for specific output functions. Different research has employed ANN to predict the biogas production from AD processes [41–44], during start-up and continuous operation [45], and to determine the composition of biogas for each process [46]. Dahunsi et al. [47] used ANN to determine the biogas yield from AD as a function of T_{op}, HRT, TS, VS, and pH. While, Holubar et al. [41] developed an ANN model to determine the potential biogas production, rate of methane production, and gas composition during the AD of lignocellulosic as a function of pH, COD, volatile fatty acids (VFAs), and VS. Yetilmezsoy et al. [48] demonstrated that an ANN can be employed to model ADs, and to determine the amount and rate of bio-fuel as a function of volumetric organic loading rate (OLR), T_{op} and substrate properties (pH, ALK, COD, and VFA). Kana et al. [49] developed an ANN model to predict the AD performance from the co-digestion of sawdust, cow dung, banana stems, rice bran, and paper waste. Behra et al. [50] confirmed that the ANN algorithm can successfully predict the percentage of methane from landfill gases. Additionally, ANN models were used to predict methane fraction, volume of biogas, effluent characteristics, gas yield, and optimum biogas production in different AD processes [51–57]. A review of relevant literature found that ANN is an effective tool to model and predict the effect of different operational parameters on the biogas production by AD under mesophilic or thermophilic conditions. Once the effects of the parameters are established biogas production can be improved by optimizing the parameters under favorable digestion conditions.

Based on the aforementioned literature review, it can be seen that AD can be used to convert the huge volumes of ASWs and CM to useful products(biogas and fertilizers); an optimized AD process for the treatment of ASWs and CM under various mixing ration, different COM_{sub}, %MC, TS, VS, Bio_{sub}, C:N ratio and HRT is crucial; there is a gap in knowledge regarding the effect of process key operational parameters on the AD performance, and a well-established model to predict and optimize the AD process under different operational conditions require further investigation. Accordingly, this paper evaluates the influence of co-digestion of ASWs and cow Manure (CM), and the chemical pre-treatment of the substrate with $NaHCO_3$ on the performance of AD and introduces predictive models conceptualized on ANNs to model, control and address the production of biogas from AD process fed with the chemically treated co-digested substrate under mesophilic and thermophilic conditions. The developed model can identify the optimum T_{op}, chemical dose (D), $COMP_{sub}$, and HRT for maximum biogas production and used to optimize the AD performance using limited experimental data. The developed ANN model is also capable of forecasting the AD performance under unexamined conditions, which saves both time and energy.

2. Materials and methods

2.1. Analytical methods

Samples analysis were conducted as per the procedures outlined in Standard Methods for the Examination of Water and Wastewater unless otherwise noted [58]. Total solids (TS) and volatile solids (VS) were measured as per test # 2450. Ammonia (NH_3) VFAs were determined as per the procedures # 4500D and # 5560, respectively. During the ammonia test, the substrate was centrifuged for 15 min at 5000 rpm in Avanti JXN-30 Series centrifuge (life science, USA) and the collected liquid was used in the test. A Hewlett Packard gas chromatography (GC-FID) (HP 68050 series Hewlett Packard, USA) was used for VFA tests. The produced biogas was collected in a 500 L plastic bags (Puxin, China), and the CMP was measured at 25 °C using water displaced methods as presented by Almomani [59]. The composition of biogas was determined in Agilent GC-TCD (Agilent technology, Model number 7890A, USA) equipped with 45–60 mesh matrix molecular sieve column (Sigma-Aldrich, St. Louis, MO, USA). The concentrations of protein and Humic acid were measured as per the procedure presented in previous work [25]. The elemental contents of the substrates (carbon, oxygen, hydrogen nitrogen and sulfur) were determined using Vario CHNS analyzer (Elementar Analysensysteme GmbH, Germany).

2.2. Substrates composition

The ASWs used in feeding the AD contain clover, grass, and wheat straw collected from a cattle farm in Qatar, and store at 4 °C until used for testing. CM was collected from a cattle farm in Qatar and used as received. The manure was stored at 4 °C to inhibit biological activity. Table 1 presents the characteristics of ASWs and CM Feedstock

2.3. Preparation of substrates

The feed to anaerobic digesters consists of ASWs mixed with CM. Initially, the ASW was cut into small pieces (1.5–2.5 mm) and left to dry in the sun for weeks. The ASW was ground to small pieces (0.25 mm) using Mortar grinder (RM 200, USA). Then, the ASWs was mixed with CM and digested within 1 month of preparation to decrease the effect of seasonal variation. The portions of the AWS and CM were calculated to produce substrates with balanced composition in terms of DSs, organic matter (OM), and nutrients and total ammonia in the range of 130 to 560 mg/L [60]. Accordingly, in this study, five reactors were operated with different ratios of ASWs:CM, primarily, R1(0:100), R2(30:70), R3(50:50), R4(70:30) , and R5(0:100). Table 2 exemplifies the reactors with different substrate compositions (COM_{sub}) which were tested at different T_{op} and chemical treatment doses (D). An analytical grade of sodium bicarbonate ($NaHCO_3$, 99%; purchased from Merck, located in Qatar) was used in the chemical pre-treatment.

2.4. Experimental procedure

Batch AD tests were used to study the CMP from the co-digestion of ASWs and CM under mesophilic and thermophilic conditions. Tests were carried out in 2.5 L lab-scale jacketed bioreactors equipped with mechanical mixers, feeding, and sampling ports. The reactors were filled with a mixture of ASWs and CM, substrate (S) to inoculum (I) ratio of 0.5 gVS/gVS, pH of 7.5 and co-digested under controlled temperature for 30 days. Each digester has different ratios of ASWs and CM based on VS as shown in Table 2. Another set of experiments was conducted, in the same reactors, for chemically treated substrate under different doses of $NaHCO_3$ (D1 = 0.25, D2 = 0.75, D3 = 1.00, D4 = 1.50 g $NaHCO_3$/g of VS).

2.5. Artificial neural network model

The ANN structure simulates linear and non-linear systems by combining and reasoning the effect of the process element on the output function. It considered a simple and fast methodology at predicting different processes performance in comparison with complicated physically related models. Within the ANN, experimental data at different process parameters, defined as input data (ID), are introduced into the model to generate a mathematical relationship of the process response (output data (OD)) without the need for a prior physical relationship. The independent and dependent process parameters are interconnected within the ANN via nodes entitled neutrons (*Neus*). The transfer function (TF) allows *Neus* to receive, store, and manipulate one or more input signals (IS) at varying intensities based on the effect of the ID and contribute to the OD. The prediction of the ANN model can be refined using error amendment learning algorithm such as feedforward-back propagation neural network (FF-BPNN)

The FF-BPNN allows for quicker forecast and correction of any abnormality or drawbacks (i.e. over-estimation or error correction) within the ANN. The FF-BPNN refine the ANN prediction by manipulating the flow of ID within the ANN layers (input layer [IL], hidden layer [HL], and output layer [OL]). The *Neus* are connected between layers by the connection weights (CW_{ij}) that are attuned following the mapping competency of the trained network and activated by a bias value (β_j). Accordingly, IL transfer the effect of the ID (X_i) to the HLs to identify the correlation between process parameters. The number of HLs depends on the process and the available data sets. In different processes, a single HL design is typical for structuring a network as it is easy to handle and creates a simple estimation of the data set. The OL is responsible for providing the network response to the user.

Initially, the forward process introduces the ID to the ANN model at the IL. The calculated CW_{ij} of the ID pass to the HL and the sum of the weighted output ($\Sigma X_i\ Cw_{ij}$) is added to a threshold bias and transferred to OL via *Neus*. Once the data signal is received at the OL, the results are compared to the experimental values and the error is subsequently calculated. Following that, the error data signal is sent backward from the OL to the IL through the HL. During training the weights and bias at each *Neu* of the back propagated signals are renewed to reduce the error signal. An *epoch* occurs when the training vectors with a single step are used to update the weights within the ANN. This iterative approach at differing *epoch* continues to update the network's weight in different vectors using the Levenberg-Marquardt training algorithm (L-M − TA)

Table 1
Characteristics of ASWs and CM Feedstock.

Feed Stock	Fixed carbon ± St Dev. (%)	Ash content (%)	Heating Value (MJ/kg			pH	Total Alkalinity mg $CaCO_3$/L	MC (%)	VS (%)	TP (g/L)	TN (g/L)
			Lower	Average	Higher						
CM	35.52 ± 0.05	13.5 ± 0.5	14.2 ± 0.6	14.4 ± 0.3	14.9 ± 0.3	6.8 ± 0.2	220 ± 1	83.30 ± 0.4	77.74 ± 0.05	20 ± 3	130 ± 5
ASWs	43.16 ± 0.02	2.5 ± 0.2				6.9 ± 0.3	1430 ± 8	8.46 ± 0.1	65.30 ± 0.07	15 ± 3	80 ± 5
Clover	42.04 ± 0.02	2.8 ± 0.5	18.0 ± 0.6	19.1 ± 0.1	20.1	6.8 ± 0.2	1120 ± 10	14.0 ± 0.8	71.2 ± 0.05	18 ± 2	100 ± 5
Grass	44.20 ± 0.05	2.4 ± 0.2	13.2 ± 0.3	14.1 ± 0.3	16.2	6.9 ± 0.2	1277 ± 5	9.1 ± 0.9	66.2 ± 0.08	13 ± 2	60 ± 4
Wheat Straw	44.20 ± 0.08	3.7 ± 0.5	14.0 ± 0.6	15.2 ± 0.2	16.0	6.95 ± 0.2	1050 ± 4	11.0 ± 0.7	66.1 ± 0. 4	15 ± 2	75 ± 5

Table 2
Experimental matrix of anaerobic reactors with different substrate composition (COM_{sub}) operated at differing operating temperatures (T_{op}) and chemical treatment doses (D).

Substrate	Temperature (°C)				Basis treatment (g $NaHCO_3$/g of VS)			
	35	45	50	55	0.25	0.75	1.00	1.5
R1 %CM = 100% %ASWs = 0%	√	√	√	√	√	√	√	√
R2 %CM = 30 %ASWs = 70	√	√	√	√	√	√	√	√
R3 %CM = 50 %ASWs = 50	√	√	√	√	√	√	√	√
R4 %CM = 70 %ASWs = 30	√	√	√	√	√	√	√	√
R5 %CM = 0 %ASWs = 100	√	√	√	√	√	√	√	√

until the error between the calculated and experimental values reaches a minimum. After effective completion of training, the ANN architecture is tested with another set of data (i.e. testing data) to confirm the process prediction ability. If the testing error is within the acceptable limit, the ANN architecture can be frozen and used to calculate the process parameter using a new ID.

In the present study, the CMP can be represented as a function of COM_{sub}, T_{op}, chemical treatment doses (D), and HRT as per Eq. (1).

$$CMP = f(\text{COMsub, Top, D, HRT}) \quad (1)$$

where CMP is cumulative methane production (NL/kgVS), COM_{sub} is the composition of the substrate, T_{op} is operating temperature, D is the dose of the $NaHCO_3$ (g/ gVS), and HRT is the hydraulic retention time (day). The configuration of the ANN used in this study is presented in Fig. 1. The input variables (COM_{sub}, T_{op}, D, HRT) were represented by four *Neus*. The output layer contains one *Neu* representing the CMP. The mathematical manipulations of the ANN were carried out using MATLAB® software (MathWork, Inc.,Version: R2010a). The optimization of the ANN was carried out following L-M−TA, where the back-propagation algorithm was used to correct and adjust the weights and bias values. In this study, a total of 6886 input data were used from 42 tests of CMP as a function of time under different conditions. The experimental data were separated into the training set, testing, and validation subsets. The ID used in the training set was representative of 56% of the data points (3856 points), while 1914 (~27.7%) data points were used in the testing set, and the remaining 1116 data points were used for validation (16.2% of the total data sets). The experimental ID data of CPM were normalized to 0.1 to 0.9 with respect to minimum/maximum values, before feeding into the ANN to facilitate the training, testing, and validation, and reduce the chance for local minima. Previous studies have demonstrated that the best practice in the ANN structure is the formulation of TFs that simulate the data sets with limited errors. This is achievable by assigning *logsig*, *tansig*, and *purelin* TFs and changing the number of *Neus* in the hidden layer. In this context, the *logsig* TFs generate an expression for the output of the *Neu* while *purelin* TFs generate the OD as demonstrated in Eqs. (2) and (3), respectively.

$$Output\ of\ the\ neutron = \frac{1}{1 + \exp(-KN_i)} \quad (2)$$

$$Output\ of\ the\ \text{purelin} = KN_i \quad (3)$$

2.6. Statistical analysis

The statistical significance of process parameters (T_{op}, chemical dose (D), $COMP_{sub}$, and HRT) on the CMP was assessed using the student's paired *t*-test. The one-way analysis of variance (ANOVA) tests were carried out at a significance level of 5% using GraphPad statistics software (Version 7.04, USA).

The training and testing of the ANN along with CW_{ij} were used to

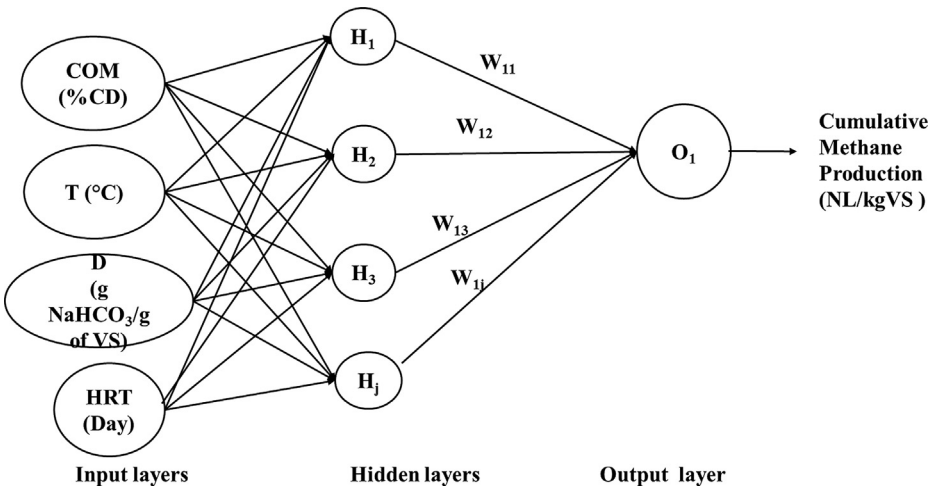

Fig. 1. Configuration of the ANN for the CMP of biogas in the co-digestion process.

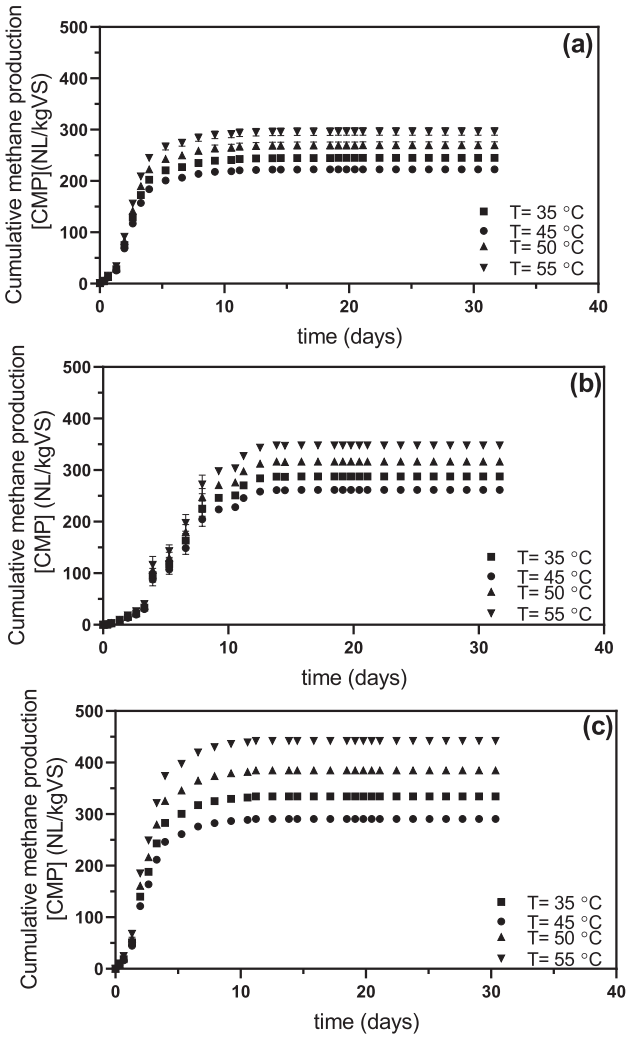

Fig. 2. Cumulative methane production (CMP) in (a) R1 (100% of CM), (b) R2 (30% CM, 70% ASWs), and (c) R4 (70% CM, 30% ASWs) at different temperatures.

predict the CMP by minimizing the error between the predicted and actual OD. This was assessed by using the root mean square (RMS) method, as per Eq. (4).

$$RMS = \sqrt{\frac{\sum CMP_{exp} - CMP_{cal}}{N \sum CMP_{exp}^2}} \tag{4}$$

where CMP_{exp} is the CMP achieved experimentally, CMP_{cal} is the CMP calculated from the ANN algorithm and N the number of data. The RMS was calculated for the training and testing data set separately. The RSM error for CMP was set in the range of 10^{-9} and 10^{-7} with the best target achieved around 10^{-8}. Subsequently, the developed model was used with the testing data to ensure that the weights and bias were at a minimal effective error (ER), as per Eq. (5).

$$ER = Max[RSM_{training}, RSM_{testing}] \tag{5}$$

where ER is the Effective error, $RSM_{training}$ is the RMS of the training data, and $RSM_{testing}$ is the RMS of the testing data. Additionally, the determination coefficient (R^2), and average absolute relative error (Ab_{RE}) outlined in Eqs. (6) and (7) were used as an indication of the predictability of the trained ANN model.

$$R^2 = 1 - \frac{\sum_{i=1}^{m} (CMP_{exp} - CMP_{cal})^2}{\sum_{i=11}^{m} (CMP_{exp} - CMP_{cal})^2} \tag{6}$$

$$Ab_{RE} = \frac{1}{N} \sum_{i=1}^{N} \left| \frac{CMP_{exp} - CMP_{cal}}{CMP_{exp}} \right| x100 \tag{7}$$

The sensitivity (SEN) of each input variable in the ANN was calculated as per Eq. (8).

$$SEN = \frac{\sum_{m=1}^{m=N_h} ((|w_{jm}^{ih}| \tilde{A} \cdot \sum_{k=1}^{N_i} |w_{km}^{ih}|) x |w_{mm}^{ho}|)}{\sum_{k=1}^{k=nI} \{\sum_{m=1}^{m=N_h} ((|w_{jm}^{ih}| \tilde{A} \cdot \sum_{k=1}^{N_i} |w_{km}^{ih}|) x |w_{mm}^{ho}|)\}} \tag{8}$$

where SEN is sensitivity or the effect of j^{th} ID on the process outcome, N_i is the number of input *Nues*, N_h is the number of hidden *Neus*, W is the connection weights. The letters 'i', 'h', and 'o' are corresponding to IL, HL, and OL, respectively. The counters 'k', 'm', and 'n' reflect the neutrons in the IL, HL, and OL, respectively.

Once the ANN architecture was frozen, it was validated with 1116 ID new data set sets different from the training or testing data sets. The frozen ANN was used after that to simulate and predict the CMP trends under unexamined conditions.

2.7. Biodegradability of the substrate

The Anaerobic biodegradability (ABD) of the substrate was calculated using Eq. (9).

$$\%AD_{biodeg} = \frac{SM}{TM} \tag{9}$$

where TM is the theoretical methane potential of the substrate calculated following Eq. (10).

$$TM = \frac{930xC + 2790xH - 350xO - 600xN - 175xS}{C + H + O + N + S} \tag{10}$$

where C, H, O, N, and S are the percentage of carbon, hydrogen, oxygen, nitrogen, and sulfur in the substrate on a dry basis, SM is the specific methane production, calculated following Eq. (11).

$$SM = \frac{VM}{gVS} \tag{11}$$

where VM is the total volume of methane produced from the substrate (NL), and gVS is the mass of volatile solids in the reactor.

3. Results and discussion

3.1. Biogas production

Fig. 2 demonstrates an example of the cumulative methane production (CMP) for the studied reactors (R1 to R5) fed with substrates which contained different portions of ASWs and CM. The CMP curves follow typical trends consisting of delay phase ranged from 1 to 3 days, followed by fast digestion represented by an exponential phase, starts just after the delay phase and lasts for 7–10 days, and lastly a stationary phase where the CMP rate levels off and the production of biogas stop. Koupaie et al., [61] observed similar CMP curves during the Co-AD of a mixture of juice- beverage, screen cake, and thickened sludge. Comparable trends were also reported by other studies using different substrates [62–64]. The rapid production of biogas during the exponential phase suggests a high digestion rate of the substrate which commences by initially hydrolyzing the biodegradable compounds, proceeding to the less biodegradable compounds achieving the final CMP. It is believed that the constant CMP values attained after ~10 days are due to the decrease in the concentration of biodegradable substrate available for AD. Zhang et al., [15] and Alkaya and Demirer [16] have shown that Co-AD improved biogas productivity and process stability due to the presence of high concentrations of the biodegradable compounds, balanced trace element and soluble carbohydrates. Astals et al., [17] and Rajagopal et al. [18] concluded that the biodegradability index, balanced nutrient and organic loading rate within the substrate control the production of methane and determine the

performance of AD process. Our recent experience during the Co-AD of different ratios of ASWs and CM showed that mixed substrates contain balanced C:N ratio and consistent texture of substrate (TS, VS and VFA) within reasonable %MC. These conditions offer balanced C, O, N and H content, help in reducing the chance for inhibition, and increase the reaction rate and biofuel production. Different studies have shown that a C:N ratio ~ 25 is required to produce the highest CMP [65,66]. Higher C:N implies low nitrogen content and excess carbon resulting in lower AD efficiency. Differently, low C:N implies a high chance for ammonia production that can lead to a sudden increase in the pH of the AD leading to bacterial inhibition and lower the CMP [67]. The highest CMP at a constant temperature was observed in R4 which was fed a substrate with ASWs: CM of 70:30%, followed by R3 (50:50), R2 (30:70), R1 (0:100), and R5 (100:0). At 35 °C, the CPM in R4 was 334.4. NL/kgVS followed with 320.2, 286.8, 245.4, and 220 NL/kgVS in R3, R2, R1 and R5, respectively. Likewise, Joute et al., [68] reported a maximum CMP and methane yield during the Co-AD of a mixture of cow manure (CM) and banana waste (BW) using a mixing ratio of 40%: 60% of CM: BW. The low CMP in R1 and R5 fed with the pure substrate confirms the feasibility of Co-AD over mono-AD as recommended by different authors [19,20]. The flow rate of methane in the 5 reactors was measured, wherein the maximum CH_4 generation rate was determined to be 35.70 NL/day for R4, followed by 31.04 NL/day for R3, 28.2 NmL/day for R2, 25.4 NL/day for R1, and 22.7 NL/day for R5.

There is a direct relationship between the %MC and the CMP with a general trend demonstrating the highest production for the %MC in the range of 34% to 48%, which decreased by heightening to % MC > 50%. Bollon et al. [69] showed that biochemical acetate degradation kinetics increased by 6 folds (290 mgCOD/kg to 2000 mgCOD/kg) by decreasing the %MC of the AD from 82 to 65%. The study concludes that the main reason for this enhancement is due to diffusion limitations within the substrate. Yuan et al., [70] achieved the highest biogas yield from the AD of rice straw pretreated by ammonia at a %MC of 70%. It was reported that high %MC is required to increase system stability, reduce the HRT of the AD and increase the CMP. Fujishima et al., [71] showed that carbohydrate removal efficiency, the population number of glucose consuming acidogenic bacteria and hydrogenotrophic and acetoclastic methanogenic bacteria increase by increasing the %MC in the substrate. The discrepancies between the % MC in different studies can be related to the differences in the other constituents in the substrate mainly solids, organic matter and nutrients. It was observed that the substrate with high OM exhibited an improved metabolization rate and achieved 23% to 30% higher CMP compared with raw substrates. The % CH_4 in the biogas generated from R1, R2, R3, R4, R5 were in the range of 66% to 73%, 68–77%, 67–76%, 69–74%, 68–77%, and 70% to 77%, respectively, with the rest consisting primarily of carbon dioxide. The variations in %CH_4 between the reactors are attributed to the differences in OM, %MC, TS and VS. Still, R2 to R4 showed the highest %CH_4 due to carbon and hydrogen contents in the feed. The obtained results suggest that the %CH_4 can be increased for any substrates by increasing OM and controlling the %MC in the range 34 to 48%.

Fig. 2 also indicates that all of the substrates exhibited higher CMP at T_{op} of 55 °C followed by 50 °C, 35 °C, and 45 °C. At T_{op} of 55 °C, R4 demonstrated a 15% increase in the CPM (442.0 NL/kgVS) compared with results achieved at 35 °C. The other reactors (R1, 2, 3 and 5) exhibited an increase in the range of 9.9% − 10% being 295.5, 352.0, 374.5, and 281.0 NL/kgVS for R1, R2, R3, and R5, respectively. Different studies have shown that the T_{op} of the AD enhance the degradation of the substrate and increases the CMP. However, for the substrate with high nitrogen content, increasing the T_{op} might result in the formation of a high concentration of ammonia (≥0.7 g-N/L) leading to AD inhibition. Angelidaki and Ahring [72] showed that at high loading rate decreasing the T_{op} ≤ 55 °C would increase the biogas yield and enhance the process stability and performance. Chae et al., [73] reported comparable biogas yield for tests carried out at T_{op} of 30

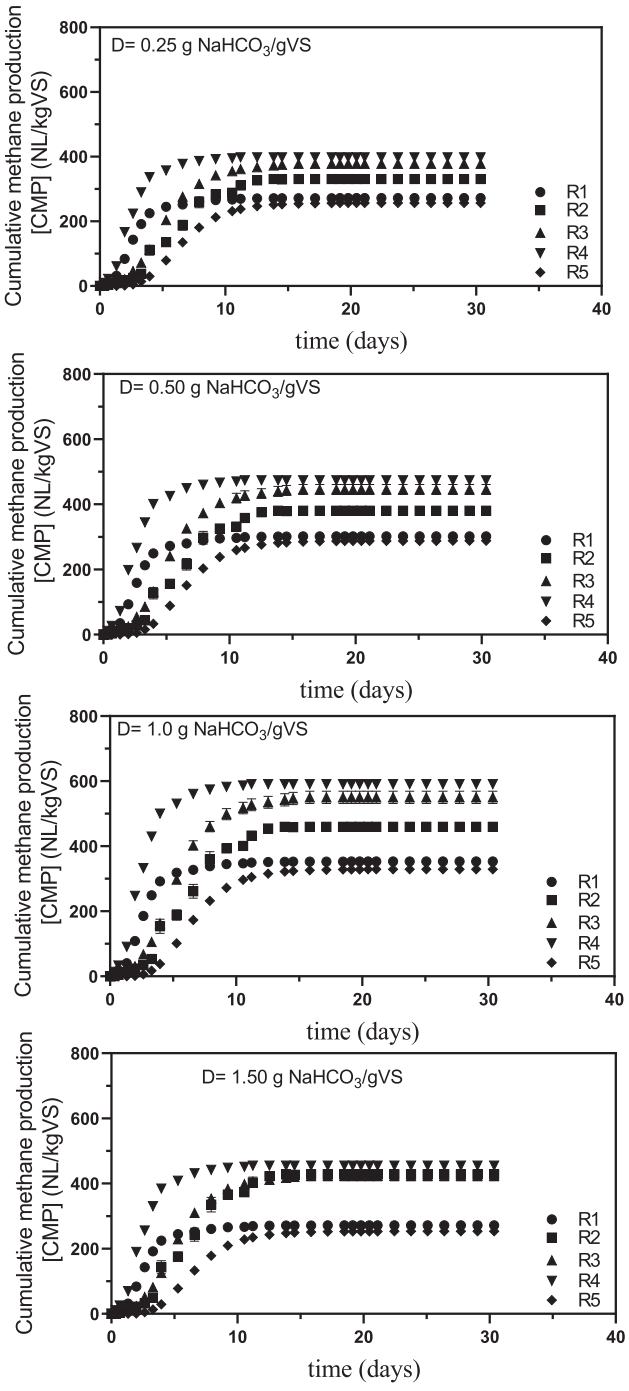

Fig. 3. Cumulative methane production (CMP) in (a) R1 (100% of CM), (b) R2 (30% CM, 70% ASWs), and (c) R4 (70% CM, 30% ASWs) at different base dosages.

and 35 °C, and a 15% reduction in the biogas yield for a test carried at T_{op} of 25 °C. Although the CMP continues to increase by increasing the T_{op}, the percentage improvement in the CMP for tests carried out at T_{op} ≥ 60 did not exceed 15%. Considering the cost of energy required to heat the AD and process complications to operate and control AD at such high T_{op}, it was decided to limit the T_{op} in the range 30 to 55 °C.

The pH, ALK, and VFA are key factors that affect the efficiency of AD. The ALK of the ASWs is 6 folds higher (1430 ± 8 mg $CaCO_3$/L) than CM (220 ± 1 mg $CaCO_3$/L). Almomani et al. [25] showed that the highest CMP was achieved for substrates with ALK in the range of 3800 to 4000 mg$CaCO_3$/L. Based on the values presented in Table 1, both ASWs and CM have low ALK value suggesting that the addition of

Table 3
Summary of the iterative tests during the training and testing of the ANN.

				Training				Testing			
Test number	# of Neu in the HL	1st TF	2nd TF	$RMS_{training}$	$\%Max_{div,\ erro}$	# ID with % $Max_{div,\ erro} > 15$	# ID with % $Max_{div,\ erro} > 10$	$RMS_{testing}$	$\%Max_{div,\ erro}$	# ID with % dev > 15	# ID with % $Max_{div,\ erro} > 10$
1	5	logsig	purelin	1.514	51.347	16.109	30.221	1.524	48.422	16.051	29.952
2	5	tansig	purelin	1.538	54.723	15.878	30.336	1.548	46.989	15.667	29.414
3	6	tansig	purelin	1.447	45.328	10.877	27.398	1.488	42.937	10.368	27.034
4	6	logsig	purelin	1.120	51.434	11.933	26.150	1.136	48.015	15.667	25.114
5	7	tansig	purelin	1.022	44.778	3.763	15.312	1.043	33.268	3.226	14.976
6	7	logsig	purelin	1.062	45.894	5.606	16.253	1.142	34.368	5.299	16.589
7	8	tansig	purelin	0.967	28.677	3.283	12.403	1.015	24.172	2.842	11.827
8	9	tansig	purelin	0.753	23.225	3.283	8.630	0.751	30.690	2.995	8.448
9	9	logsig	purelin	0.673	32.513	2.371	6.451	0.702	32.625	2.304	6.067
10	10	tansig	purelin	0.735	28.374	2.112	7.085	0.756	23.847	1.766	6.835
11	11	tansig	purelin	0.618	32.210	2.342	4.339	0.651	30.839	1.997	4.070
12	11	logsig	purelin	0.766	28.102	0.787	4.378	0.762	23.013	0.998	3.840
13	12	logsig	purelin	0.560	30.846	0.941	3.168	0.569	19.994	0.998	2.995
14	12	tansig	purelin	0.794	28.992	0.336	4.147	0.867	18.665	0.230	4.454
15	13	logsig	purelin	0.449	25.905	0.230	1.814	0.454	21.557	0.154	1.613
16	13	tansig	purelin	0.584	15.651	0.154	1.315	0.599	18.230	0.230	1.306
17	14	tansig	purelin	0.489	18.092	0.154	1.286	0.507	19.778	0.307	0.998
18	14	logsig	purelin	0.475	26.888	0.115	0.941	0.473	23.214	0.154	0.922
19	15	logsig	purelin	0.449	17.198	0.077	0.259	0.448	12.621	0.000	0.230
20	15	tansig	purelin	0.417	17.594	0.038	0.758	0.410	15.242	0.154	0.845

alkalinity might enhance the CMP from these substrates. Li et al. [74] suggested that a concentration of VFA ≥ 190 mg/L might inhibit the AD. In the present study, the concentrations of VFA for CM were in the range of 112 ± 2 to119 ± 2 mg/L with 20% propionate, 55% acetate, and the rest is butyrate. ASWs contain VFA in the range 70 ± 2 to 85 ± 2 mg/L with 30% as propionate, 48% as acetate, and the rest is butyrate. As the biodegradation of propionate is slower than acetate and butyrate [19,75], it is expected that CM should contribute more to methane production than ASWs. Ammonia which produces during the digestion of proteins, peptides, and amino acids is essential to maintain balanced C:N ratio, neutralization of VFAs, and stabilize the pH of the AD [30]. Any decrease in the concentration of ammonia in AD might lead to decrease in bacterial growth and reduction in CMP production. The $\%AD_{biodeg}$ of the feed to the reactors was increased by increasing the %ASWs in the substrate. Given that, the $\%AD_{biodeg}$ was found to be 53.40% for R5 followed by 52.0% for R4, 43.2% for R3, 40.15% for R2, and 33.42% for R1. As the maximum CMP was observed in R4, it can be concluded that a 70% of the ASWs to be the most suitable composition for maximum biogas production.

The effect of basic treatment on the CMP in the five reactors were studied at different $NaHCO_3$ doses (D1 = 0.25, D2 = 0.75, D3 = 1.00, and D4 = 1.5 g $NaHCO_3$/gVS). Fig. 3 presents the CPM as a function of time for all the reactors under different $NaHCO_3$ doses. For all of the studied reactors, applying alkalinity treatment with a dose of 1.0 g $NaHCO_3$/gVS exhibited the highest CMP. The CMP was increased by 11, 15, 18, 19, and 12% after applying D1 (0.25 g $NaHCO_3$/gVS) in R1, R2, R3, R4, and R5, respectively, while D3 (1.00 g $NaHCO_3$/gVS) demonstrated an improvement in the CMP by 44, 59, 71, 76, and 43% for the same reactors, respectively. Treatment with D4 exhibited an improvement of 10.8, 43, 32, 35, and 11%, respectively, compared with the untreated substrate. For all of the reactors, it was observed that the maximum CMP occurred during the first three days, subsequently decreasing until the end of digestion.

The enhancement in the CMP after the alkalinity treatment can be related to the ability of $NaHCO_3$ to breakdown the complex Li in the ASWs. The substrates used in the feeding of the AD process contain easy to degraded compounds (e.g. Ce and HCe) as well as complex and less biodegradable compounds (Li) [76]. Applying the chemical treatment allows the $NaHCO_3$ to attack substrate leading to the decomposition of CE and HCe to smaller compounds (i.e. improve the Bio_{sub}) *to* disintegrate the link between polysaccharide and Li and liberate the biodegradable cell content to be available for bacterial use [8,63]. Thus, the $\%AD_{biodeg}$ of the substrate increase and the CMP enhanced. The disintegration of the solids in the substrate was verified by the increase in the soluble COD content and the decrease in the TS of the substrate. The TS content of the substrate was decreased by 3.1–7.1%, 8.5–12.9%, 10.9–16.3%, 15.9–23.5%, and 13.5–18.6% for reactors R1, R2, R3, R4, and R5, respectively. Soluble chemical oxygen demand (CODs) was increased from 3 to 5 fold, 6 to 8 fold, 12 to 15 fold, and 9 to 10 fold after the treatment with D1, D2, D3, D4, and D5, respectively. Tian [77] confirmed that alkalinity treatment disintegrates the substrate cells, liberate the biodegradable OMs, and improves the performance of AD. Zhang [62] reported that methane (CH_4) is produced in the AD from Li, CE, and HCe as the main source of carbon. Accordingly the efficiency of AD and the reported CMP increased. Moreover, treatment with a base can help stabilize the pH in the AD and improve its performance. The decrease in the CMP at D5 was related to the disturbance in the reactor buffering capacity that might have affected the AD performance or inhibited bacterial activity. Furthermore, at a high ALK the substrate contains fewer active microorganisms which can lead to a lower CMP. Rinzema [78] observed a 10% AD inhibition when the concentration of Na^+ in the substrate increased to 5 g/L, and total inhibition for concentration ≥ 14 g/L. The maximum concentrations of Na^+ in all the reactors did not exceed 2.77 g/L being 1.34 in R1, 1.68 in R2, 2.13 in R2, 2.45 in R3, 2.65 in R4, and 2.77 g/L in R5, suggesting that Na^+ imbibition is unlikely. Similar trends were reported by Barakat [79] and Bondesson [80]. The attained trends suggest that proper basic treatment could improve the co-digestion performance of ASWs and CM. However, overuse can cause microbe inhibition and reduce AD performance [58]. Thus, a proper base dose should be determined in relation to COM_{sub}, T_{op}, TS, and reactor design.

Various studies have reported an enhancement in the CMP, an increase in $Bio_{sub,}$ and a decrease in moisture toxicity by applying advanced oxidation processes (AOP) [25,81]. Given the high cost accompanying the application of AOPs, the co-digestion and chemical treatment with $NaHCO_3$ provides promising results for the enhancement of CMP.

The $\%AD_{biodeg}$ after applying the chemical treatment was increased to 42.42%, 51.15%, 63.2%, 76.0%, and 72.40% for R1, R2, R3, R4, and R5, respectively. The improvement in the $\%AD_{biodeg}$ and the net CMP after the chemical treatment is connected to the breakdown of cells releasing the cell contents and increasing the portion of the

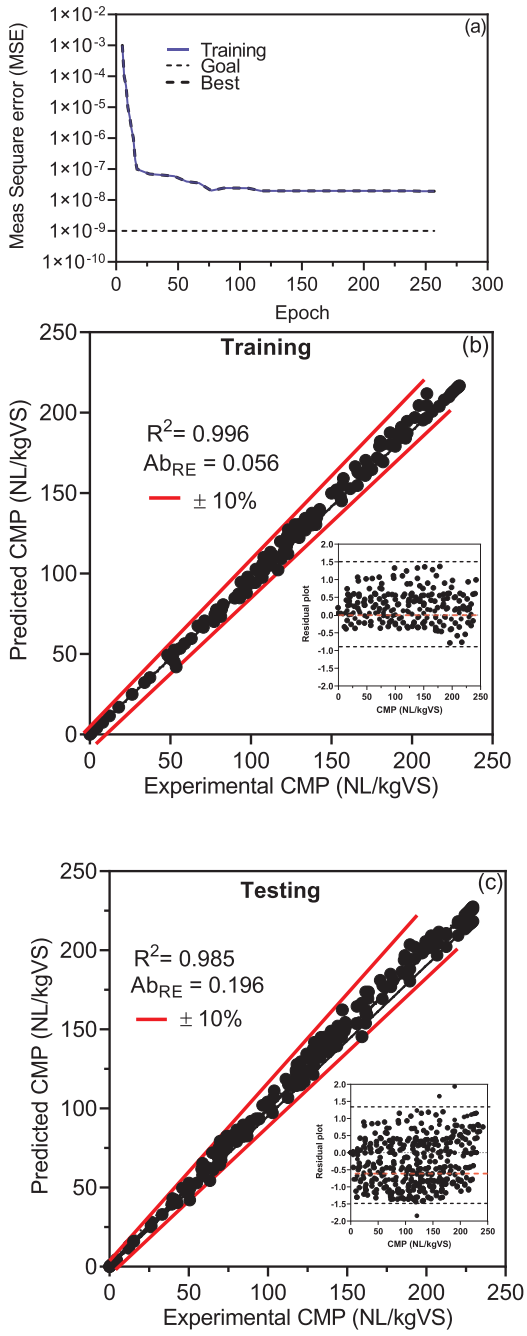

Fig. 4. (a) The change in the mean squared error vs epochs during training, (b) Experimental vs predicted CMP during training manipulation (inner: plot of residuals between experimental and predicted data), and (c) Experimental vs predicted CMP during testing manipulation (inner: plot of residuals between experimental and predicted data).

biodegradable organic matter; thus, enhancing the metabolic production of methane. The results achieved in this study were comparable with the limited results published in the relevant literature. Zheng [82] showed that the pre-treatment of a mixture of banana stems and swine manure with using 6 wt% NaOH improved the biogas and methane yield by 12.1% and 21.4%, respectively. Noonari [27] improved the methane yield produced from canola straw (CS) with buffalo manure (BD) 9.3% and 11.2% using.8 and 0.5 mg/gVs of magnetite nanoparticles (Fe_3O_4 NPs).

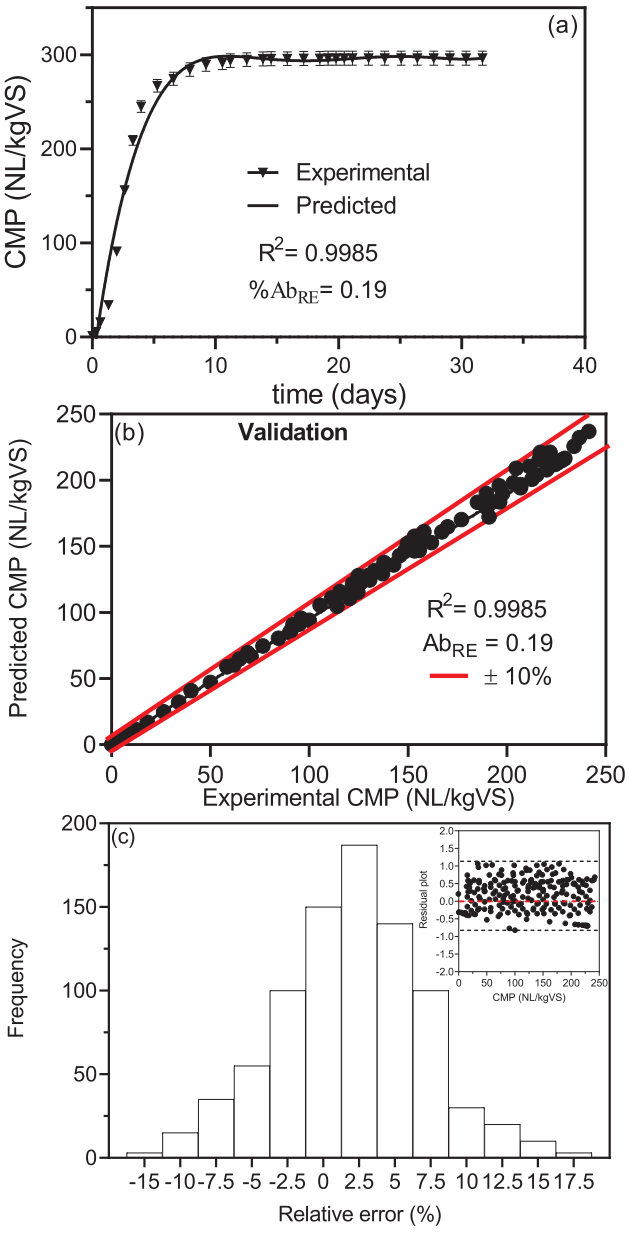

Fig. 5. (a) Experimental (dots) and predicted (solid line) CMP using the developed ANN model, (b) Experimental vs predicted CMP during validation tests, and (c) the Ab_{RE} between experimental and predicted CMP data (inner: residuals between experimental and predicted data).

3.2. Developing ANN model

Table 3 displays the results of the training and testing data fitted under different *Neus* using the *Logsig* and *purelin* transfer function. The number of *Nues* was varied until a reasonable prediction of the CMP was achieved with minimal errors. The statistical analysis for the most suitable ANN architecture was based on minimum error regarding RMS, maximum percentage deviation error ($\%Max_{div,\ erro}$), and the number of data points with various percentage deviations for training and testing data points. Different numerical trials were performed to establish the most suitable network architecture. The network was frozen when 99.5% of the predicted data fell within $\%Max_{div,\ erro}$ of ± 15% from experimental data, and at least 97% of predicted data fell within $\%Max_{div,\ erro}$ of ± 10% of the experimental data, and there was minimal RMS error for training and testing data. Table 3 indicates that following several numerical iterations, it was noted that the most suitable fit for

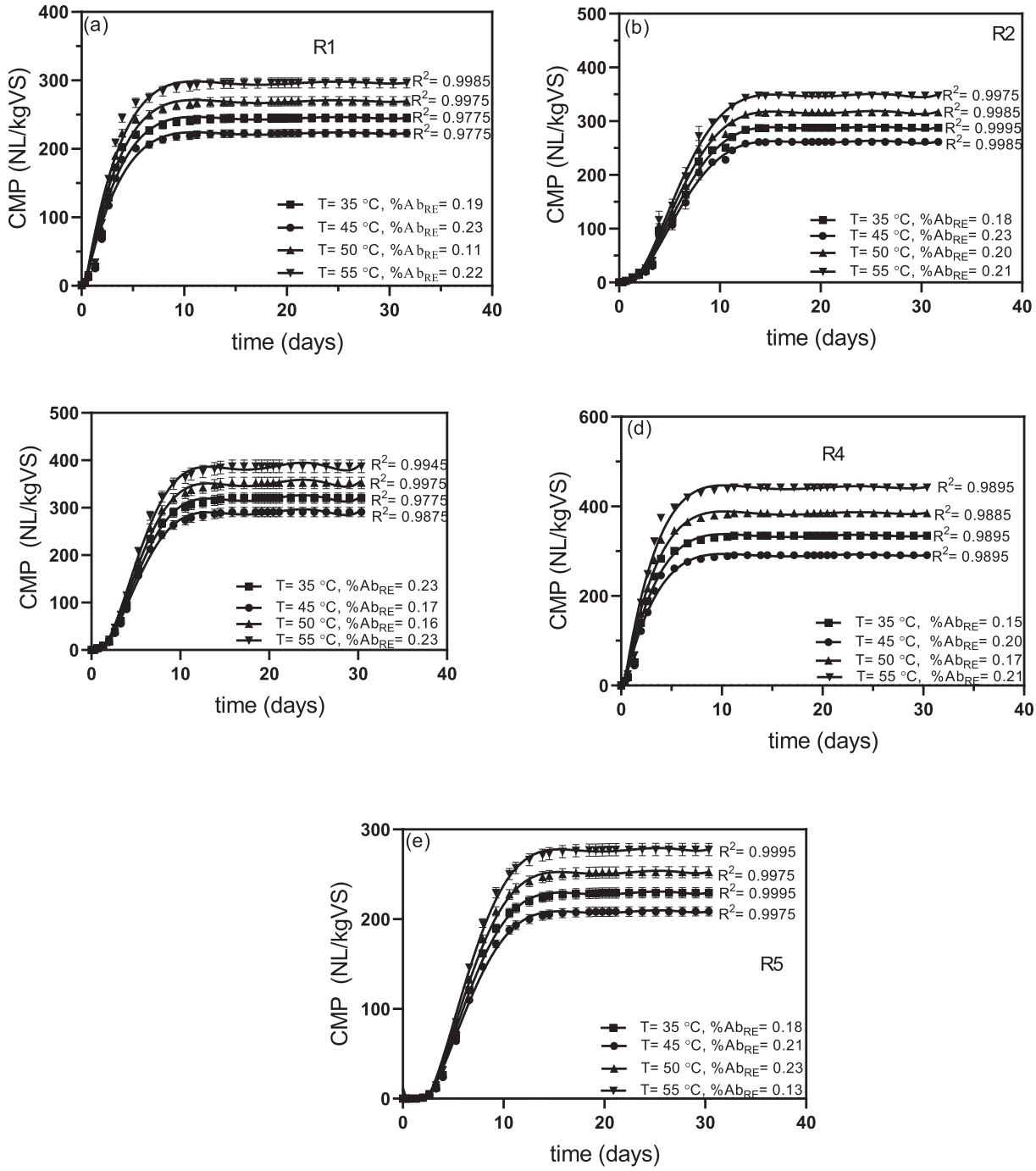

Fig. 6. Experimental and predicted CMP under different COM_{sub} and T_{op}.

the ANN was achieved when the structure consisted of a single HL and 15 *Neus*. The numerical iteration was aimed at creating the appropriate TF between the IL and HL by using the *tansig* and *logsig*. As previously suggested, the CMP curves are not linear, accordingly the TFs used in the calculations were not linear. The results indicated that the architecture that contain *logsig* TFs between the IL and the HL, and *purelin* TFs between the IL and the OL exhibited an accurate prediction of the CMP trends. The training tests with 3856 ID displayed a maximum RMS error and $\%Max_{div,\ erro}$ of 0.449% and 17.198%, respectively. The testing process with 1914 exhibited a maximum RMS error and $\%Max_{div,\ erro}$ of 0.448% and 12.621%, respectively. The calculations were repeated several times under different *epochs* to achieve the required performance goal of 10^{-9}. Fig. 4a exemplifies the change in the mean squared error as a function of the number of *epochs* during the training process. It is evident that the mean squared error decreases by elevating the number of *epochs* until 260 is reached, after which the value remains constant. This suggests that 260 is the most suitable number of *Neuts* to model the CMP. The results displayed in Table 3 and Fig. 3a indicate that an ANN which consists of three layers, with one hidden layer comprised of 15 *Neuts* and 260 *epochs* is suitable to predict the CMP with a high level of accuracy and can be used as the ANN freezing limit.

Fig. 4b and c display the plot of the calculated versus experimental CMP values following the developed ANN model during the training and testing steps. The data are scattered around a 45° line on the crosswise dotted line. This suggests a strong correlation between the experimental and calculated values. Furthermore, Fig. 4b and 4c indicate that much of the data is within ± 10% of the line of standard

Table 4
A statistical analysis between the experimental and predicted CMP under different substrate composition and operating temperatures.

Test	Temperature	R^2	$\%Ab_{RE}$	St. Dev
R1				
1	35	0.9775	0.19	6.345
2	45	0.9775	0.23	6.389415
3	50	0.9775	0.11	6.434141
4	55	0.9985	0.22	6.47918
R2				
5	35	0.9995	0.18	6.338655
6	45	0.9985	0.23	6.383026
7	50	0.9985	0.2	6.427707
8	55	0.9975	0.21	6.472701
R3				
9	35	0.9775	0.23	6.332316
10	45	0.9875	0.17	6.376643
11	50	0.9975	0.16	6.421279
12	55	0.9945	0.23	6.466228
R4				
13	35	0.9895	0.15	6.965548
14	45	0.9895	0.2	7.014307
15	50	0.98885	0.17	7.063407
16	55	0.9895	0.21	7.112851
R5				
13	35	0.9995	0.18	9.055212
14	45	0.9975	0.21	9.118599
15	50	0.9975	0.23	9.182429
16	55	0.9995	0.13	9.246706

deviation. This confirms that the selected freezing limit of the ANN applies to the current system. The statistical analysis of the data showed that during the training and testing stages up to 98.7% and 99.1% of the data points were within ± 10% deviation of the mean values, respectively. Additionally, the data indicated that up to 98.3% and 98.7% were within ± 15% deviation of the mean values, respectively. The R^2 and Ab_{RE} for the training data were 0.996% and 0.056%, respectively. Alternatively, the values were 0.985% and 0.196% for testing data, respectively. The frequency count versus the relative error was tested for the training and testing data. The results signified that the developed ANN model followed a Gaussian distribution with a relative error range between −32.6% and 33.5% and −27.8% to 30.9% for training and testing data, respectively. The inner graphs of Fig. 4b and 4c show that the plot of residuals between the experimental and predicted data are scattered around the horizontal zero line, with an error in the range of −1 to 1.5 and −1.5 to 1.6 for training and testing data, respectively. The low range of residuals suggests a very small variation between the calculated and experimental data. This confirms that the level used for freezing the ANN model is acceptable and that the ANN does not have any systematic errors. The far scattering of some of the data points from the zero line is likely due in part to the noise in the experimental data and might not be exclusively connected to the accuracy of the ANN model.

The sensitivity analysis following Eq. (8) was used to evaluate the importance of each input variable of the CMP. The relative importance was calculated by determining the percentage weight contribution of each of the parameters of the resultant CMP. The results indicated that COM_{sub} is the major contributor to the CMP with a 65.5% influence, followed by doses of 15.8%, HRT with 10.9%, and T_{op} of 7.8%.

3.3. Validation of the ANN model

The developed ANN under frozen conditions was tested with the 1116 separate data points. Fig. 5a presents the CMP along with the predicted trends. An analysis of variance (ANOVA) statistical analysis indicated that 95% of the data points (1060 points) and 91.5% (1015 points) were predicted with a $\%Max_{div,\ erro}$ of ± 7.5% and ± 10%,

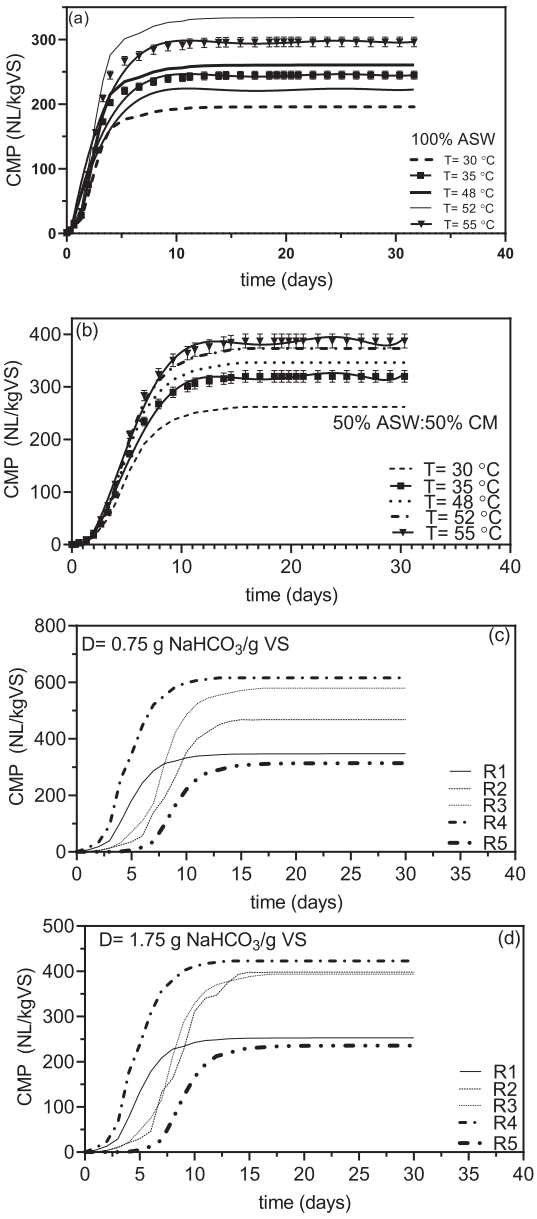

Fig. 7. Predicted CMP curves under different T_{op}, COM_{sub} and chemical treatment doses (D).

respectively. Fig. 5b presents the RMS of the error, R^2 and Ab_{RE} which were found to be 0.0035%, 0.9985% and 0.19%, respectively. The frequency counts vs. relative error for the experimental data histogram (Fig. 5c) showed that 88.7% and 99.8% of the CMP data points are within ± 7.% and ± 10% deviation, respectively. The plot of residuals between the experimental and predicted data were all scattered around the horizontal zero lines with an error in the range of −1.0 to 1.2. The results suggest a very small variation between the model and experimental data. This confirms that the level used for freezing the ANN model is acceptable.

After validating the developed ANN model, the CMP from different experimental conditions were tested against the experimental results. Fig. 6a-e present and experimental and predicted values for the five reactors, fed with different substrate compositions operated at various T_{op}. Table 4 presents the statistical significance using ANOVA. Under all conditions, the developed model predicts the experimental CMP with a high level of accuracy. The student T-test of each point at P = 05 showed a negligible significance between the experimental and predicted data. This suggests that the developed ANN model is adequately

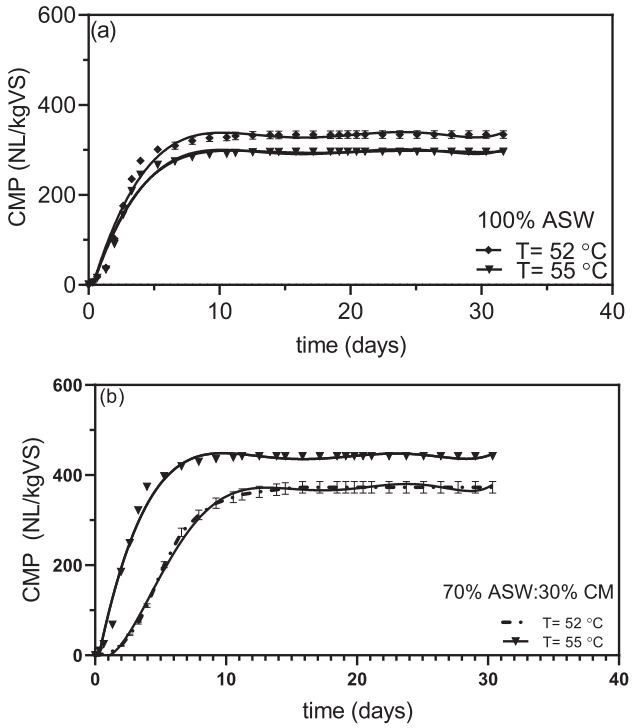

Fig. 8. Experimental and predicted CMP curves under different T_{op}, (a) 100 ASWs and (b) 70% ASWs.

able to predict the CMP as a function of different input parameters. Additionally, the ANN can be used to anticipate the CMP under different conditions, which was not previously studied experimentally. The statistical analysis also shows the accuracy of the developed model in predicting the CMP, as it reaches up to 99.5% within ± 10% of % $Max_{div,\ erro}$. Further, the ANN model can be utilized to predict the CMP as a function of T_{op}, $COM_{sub,}$ D, and HRT.

3.4. Developing CMP curves

Fig. 7a-c present the predicted CMP curves under different T_{op}, two different COM_{sub} (100% and 50% ASWs with balanced CM), and two different doses (0.75 and 1.75 g$NaHCO_3$/g.VS). The predicted CMP curves, under all conditions, displayed identical shapes to those observed experimentally. At a constant temperature, the CMP begins to exponentially increase, after a lag phase of 1 to 2 days, up to the maximum value which was identified as the ultimate CMP. Additionally, the CMP varied at different COM_{sub} and T_{op}. For example, Fig. 7a exhibits how the reactor fed with 100% ASWs has the highest CMP at 52 °C, followed by 48 °C, 35 °C, and 30 °C. Moreover, the CMP produced by the co-digested substrate (50% ASWs) exemplified the highest CMP at 55 °C, followed by 52 °C, 48 °C, 35 °C, and 30 °C. Fig. 7c and d indicate that the CMP increases by treating the substrate with 0.75 g of $NaHCO_3$ and decreases at higher doses. Additionally, the Fig. 7c and d highlight that the developed model can be used to predict the CMP at any HRT during the substrate digestions. For all the studied conditions it was observed that the CMP reached a constant CMP after ~ 10 days, thus, it is highly recommended to cut off the HRT of the AD process to this time. Shorten the HRT will have a significant positive impact on the feasibility of the AD process, as one reactor can be used three times per month to convert agricultural solid wastes for biofuel and fertilizers. Substrate composition (COM_{sub}), operating temperature (T_{op}), doses (D), and hydraulic retention time (HRT) were tested and the developed model exhibited excellent predictability under all of these conditions. The maximum CMP was reported in the range 50–55 °C, which was predicted by the developed ANN model, and verified by performing experiments under similar conditions as presented in Fig. 8a and b.

4. Conclusion

A process was proposed to improve the performance of AD and increase the CMP by co-digestion and chemical pre-treatment of the substrate. Co-digestion of ASWs and CM at a ratio of 70:30 at $T_{op} \leq 55$ °C and %MC in the range of 34% to 48% increased the CMP by at least 23% compared with raw substrates. Applying $NaHCO_3$ chemical treatment to the substrate degraded solids to smaller compounds, disintegrate the link between polysaccharide and lignin, and improved the substrate biodegradability by at least 43% leading to higher AD rate. Up to 591 NL/kgVS CMP was achieved by using 1 g $NaHCO_3$/gVS. An artificial neural network architecture consisting of three layers, 15 neutrons, and 260 *epochs* was developed and showed high accuracy predicting the AD process performance under different operational conditions. The ANN result revealed that the COM_{sub}, the chemical $NaHCO_3$ dose, HRT, and T_{op} are the main process parameter that contributes to the AD process and can be manipulated to enhance its performance. As such, the study confirms the capacity of the ANN model to predict the behavior of AD and identify the optimum conditions in a short time.

CRediT authorship contribution statement

Fares Almomani: Conceptualization, Data curation, Formal analysis, Methodology, Project administration, Software, Validation, Writing - original draft, Writing - review & editing.

Declaration of Competing Interest

The authors declare that they have no known competing financial interests or personal relationships that could have appeared to influence the work reported in this paper.

References

[1] Efome JE, Rana D, Matsuura T, Lan CQ. Effects of operating parameters and co-existing ions on the efficiency of heavy metal ions removal by nano-fibrous metal-organic framework membrane filtration process. Sci Total Environ 2019;674:355–62.
[2] Rajendran K, Mahapatra D, Venkatraman AV, Muthuswamy S, Pugazhendhi A. Advancing anaerobic digestion through two-stage processes: Current developments and future trends. Renew Sustain Energy Rev 2020;123:109746.
[3] Salameh T, Tawalbeh M, Al-Shannag M, Saidan M, Melhem KB, Alkasrawi M. Energy saving in the process of bioethanol production from renewable paper mill sludge. Energy 2020;196:117085.
[4] Tawalbeh M, Rajangam AS, Salameh T, Al-Othman A, Alkasrawi M. Characterization of paper mill sludge as a renewable feedstock for sustainable hydrogen and biofuels production. Int J Hydrogen Energy 2020.
[5] Sun J, Peng H, Chen J, Wang X, Wei M, Li W, et al. An estimation of CO_2 emission via agricultural crop residue open field burning in China from 1996 to 2013. J Cleaner Prod 2016;112:2625–31.
[6] Ni H, Han Y, Cao J, Chen LWA, Tian J, Wang X, et al. Emission characteristics of carbonaceous particles and trace gases from open burning of crop residues in China. Atmos Environ 2015;123:399–406.
[7] Padula DJ, Madigan TL, Nowak BF. Australian farmed Yellowtail Kingfish (Seriola lalandi) and Mulloway (Argyrosomus hololepidotus): Residues of metallic, agricultural and veterinary chemicals, dioxins and polychlorinated biphenyls. Chemosphere 2012;86(7):709–17.
[8] Chen G-y, Zheng Z, X-x ZOU, J-h LI, S-g YANG. Anaerobic Co-digestion of Rice Straw and Swine Feces. J Agro-Environ Sci 2009;1.
[9] Song C, Yuan W, Shan S, Ma Q, Zhang H, Wang X, et al. Changes of nutrients and potentially toxic elements during hydrothermal carbonization of pig manure. Chemosphere 2020;243:125331.
[10] Zhang N, Zheng H, Hu X, Zhu Q, Stanislaus MS, Li S, et al. Enhanced bio-methane production from ammonium-rich waste using eggshell-and lignite-modified zeolite (ELMZ) as a bio-adsorbent during anaerobic digestion. Process Biochem 2019;81:148–55.
[11] Krishnan S, Singh L, Sakinah M, Thakur S, Wahid ZA, Alkasrawi M. Process enhancement of hydrogen and methane production from palm oil mill effluent using two-stage thermophilic and mesophilic fermentation. Int J Hydrogen Energy 2016;41(30):12888–98.

[12] Nogueira RGS, Lim TT, Wang H, Rodrigues PHM. Performance, microbial community analysis and fertilizer value of anaerobic co-digestion of cattle manure with waste kitchen oil. Appl Eng Agric 2019;35(2):239–48.
[13] Imeni SM, Pelaz L, Corchado-Lopo C, Busquets AM, Ponsá S, Colón J. Techno-economic assessment of anaerobic co-digestion of livestock manure and cheese whey (Cow, Goat & Sheep) at small to medium dairy farms. Bioresour Technol 2019;291:121872.
[14] Zhang X, Gu J, Wang X, Zhang K, Yin Y, Zhang R, et al. Effects of tylosin, ciprofloxacin, and sulfadimidine on mcrA gene abundance and the methanogen community during anaerobic digestion of cattle manure. Chemosphere 2019;221:81–8.
[15] Zhang L, Lee Y-W, Jahng D. Anaerobic co-digestion of food waste and piggery wastewater: Focusing on the role of trace elements. Bioresour Technol 2011;102(8):5048–59.
[16] Alkaya E, Demirer GN. Anaerobic mesophilic co-digestion of sugar-beet processing wastewater and beet-pulp in batch reactors. Renewable Energy 2011;36(3):971–5.
[17] Astals S, Nolla-Ardèvol V, Mata-Alvarez J. Thermophilic co-digestion of pig manure and crude glycerol: process performance and digestate stability. J Biotechnol 2013;166(3):97–104.
[18] Rajagopal R, Massé DI, Singh G. A critical review on inhibition of anaerobic digestion process by excess ammonia. Bioresour Technol 2013;143:632–41.
[19] Xu F, Li Y, Ge X, Yang L, Li Y. Anaerobic digestion of food waste–Challenges and opportunities. Bioresour Technol 2018;247:1047–58.
[20] Sahito A, Mahar R. Enhancing methane production from rice straw co-digested with buffalo dung by optimizing effect of substrate ratio, alkaline doze and particle size. J Anim Plant Sci 2014;24(4):1076–84.
[21] Lalak J, Kasprzycka A, Martyniak D, Tys J. Effect of biological pretreatment of Agropyron elongatum 'BAMAR' on biogas production by anaerobic digestion. Bioresour Technol 2016;200:194–200.
[22] Al Momani F, Schaefer S, Sievers M. Improved sludge dewaterability for sequential ozonation–aerobic treatment. Ozone Sci Eng 2010;32(4):252–8.
[23] Al Momani F, Schaefer S, Sievers M. Effect of ozone pre-treatment on sludge production of aerobic digestion processes. Int J Sustain Eng 2011;4(02):181–9.
[24] Atelge MR, Atabani AE, Banu JR, Krisa D, Kaya M, Eskicioglu C, et al. A critical review of pretreatment technologies to enhance anaerobic digestion and energy recovery. Fuel 2020;270:117494.
[25] Almomani F, Bhosale R, Khraisheh M, Shawaqfah M. Enhancement of biogas production from agricultural wastes via pre-treatment with advanced oxidation processes. Fuel 2019;253:964–74.
[26] Zhen G, Lu X, Kato H, Zhao Y, Li Y-Y. Overview of pretreatment strategies for enhancing sewage sludge disintegration and subsequent anaerobic digestion: Current advances, full-scale application and future perspectives. Renew Sustain Energy Rev 2017;69:559–77.
[27] Noonari A, Mahar R, Sahito A, Brohi K. Anaerobic co-digestion of canola straw and banana plant wastes with buffalo dung: Effect of Fe_3O_4 nanoparticles on methane yield. Renewable Energy 2019;133:1046–54.
[28] Gerardi MH. The microbiology of anaerobic digesters. John Wiley & Sons; 2003.
[29] Bharathiraja B, Sudharsanaa T, Bharghavi A, Jayamuthunagai J, Praveenkumar R. Biohydrogen and Biogas–An overview on feedstocks and enhancement process. Fuel 2016;185:810–28.
[30] Benabdallah El Hadj T, Astals S, Gali A, Mace S, Mata-lvarez J. Ammonia influence in anaerobic digestion of OFMSW. Water Sci Technol 2009;59(6):1153–8.
[31] Sambo A, Garba B, Danshehu B. Effect of some operating parameters on biogas production rate. Renewable Energy 1995;6(3):343–4.
[32] Mahanta P, Dewan A, Saha U, Kalita P. Influence of temperature and total solid concentration on the gas production rate of biogas digester. J Energy Southern Africa 2004;15(4):112–7.
[33] Maroušek J. Prospects in straw disintegration for biogas production. Environ Sci Pollut Res 2013;20(10):7268–74.
[34] Ye J, Li D, Sun Y, Wang G, Yuan Z, Zhen F, et al. Improved biogas production from rice straw by co-digestion with kitchen waste and pig manure. Waste Manage 2013;33(12):2653–8.
[35] Nguyen LN, Nguyen AQ, Johir MAH, Guo W, Ngo HH, Chaves AV, et al. Application of rumen and anaerobic sludge microbes for bio harvesting from lignocellulosic biomass. Chemosphere 2019;228:702–8.
[36] Yang M, Lu D, Yang J, Zhao Y, Zhao Q, Sun Y, et al. Carbon and nitrogen metabolic pathways and interaction of cold-resistant heterotrophic nitrifying bacteria under aerobic and anaerobic conditions. Chemosphere 2019;234:162–70.
[37] Zhou Y, Guo B, Zhang L, Zou X, Yang S, Zhang H, et al. Anaerobically digested blackwater treatment by simultaneous denitrification and anammox processes: Feeding loading affects reactor performance and microbial community succession. Chemosphere 2020;241:125101.
[38] Yusuf M, Debora A, Ogheneruona D. Ambient temperature kinetic assessment of biogas production from co-digestion of horse and cow dung. Res Agric Eng 2011;57(3):97–104.
[39] Syaichurrozi I, Sumardiono S. Biogas production kinetic from vinasse waste in batch mode anaerobic digestion. World Appl Sc J 2013;26(11):1464–72.
[40] Wang J, Wan W. Kinetic models for fermentative hydrogen production: a review. Int J Hydrogen Energy 2009;34(8):3313–23.
[41] Holubar P, Zani L, Hager M, Fröschl W, Radak Z, Braun R. Advanced controlling of anaerobic digestion by means of hierarchical neural networks. Water Res 2002;36(10):2582–8.
[42] Akbaş H, Bilgen B, Turhan AM. An integrated prediction and optimization model of biogas production system at a wastewater treatment facility. Bioresour Technol 2015;196:566–76.
[43] Dibaba OR, Lahiri SK, T'Jonck S, Dutta A. Experimental and artificial neural network modeling of a Upflow Anaerobic Contactor (UAC) for biogas production from Vinasse. Int J Chem Reactor Eng 2016;14(6):1241–54.
[44] Betiku E, Okunsolawo SS, Ajala SO, Odedele OS. Performance evaluation of artificial neural network coupled with generic algorithm and response surface methodology in modeling and optimization of biodiesel production process parameters from shea tree (Vitellaria paradoxa) nut butter. Renewable Energy 2015;76:408–17.
[45] Holubar P, Zani L, Hager M, Fröschl W, Radak Z, Braun R. Start-up and recovery of a biogas-reactor using a hierarchical neural network-based control tool. J Chem Technol Biotechnol: Int Res Process Environ Clean Technol 2003;78(8):847–54.
[46] Strik DP, Domnanovich AM, Zani L, Braun R, Holubar P. Prediction of trace compounds in biogas from anaerobic digestion using the MATLAB Neural Network Toolbox. Environ Modell Software 2005;20(6):803–10.
[47] Dahunsi S, Oranusi S, Owolabi J, Efeovbokhan V. Comparative biogas generation from fruit peels of fluted pumpkin (Telfairia occidentalis) and its optimization. Bioresour Technol 2016;221:517–25.
[48] Yetilmezsoy K, Turkdogan FI, Temizel I, Gunay A. Development of ann-based models to predict biogas and methane productions in anaerobic treatment of molasses wastewater. Int J Green Energy 2013;10(9):885–907.
[49] Kana EG, Oloke J, Lateef A, Adesiyan M. Modeling and optimization of biogas production on saw dust and other co-substrates using artificial neural network and genetic algorithm. Renewable Energy 2012;46:276–81.
[50] Behera SK, Meher SK, Park H-S. Artificial neural network model for predicting methane percentage in biogas recovered from a landfill upon injection of liquid organic waste. Clean Technol Environ Policy 2015;17(2):443–53.
[51] Jaroenpoj S, Yu J, Ness J. Development of artificial neural network models for biogas production from co-digestion of leachate and pineapple peel. Glob Environ Eng 2015;1:42–7.
[52] Barik D, Murugan S. An artificial neural network and genetic algorithm optimized model for biogas production from co-digestion of seed cake of karanja and cattle dung. Waste Biomass Valorization 2015;6(6):1015–27.
[53] Astals S, Nolla-Ardèvol V, Mata-Alvarez J. Anaerobic co-digestion of pig manure and crude glycerol at mesophilic conditions: Biogas and digestate. Bioresour Technol 2012;110:63–70.
[54] Palaniswamy D, Ramesh G, Sivasankaran S, Kathiravan N. Optimising biogas from food waste using a neural network model. Proceedings of the Institution of Civil Engineers-Municipal Engineer. 170. Thomas Telford Ltd; 2017:221-9.
[55] Sathish S, Vivekanandan S. Parametric optimization for floating drum anaerobic bio-digester using Response Surface Methodology and Artificial Neural Network. Alexandria Eng J 2016;55(4):3297–307.
[56] Nair VV, Dhar H, Kumar S, Thalla AK, Mukherjee S, Wong JW. Artificial neural network based modeling to evaluate methane yield from biogas in a laboratory-scale anaerobic bioreactor. Bioresour Technol 2016;217:90–9.
[57] Li H, Ke L, Chen Z, Feng G, Xia D, Wang Y, et al. Estimating the fates of C and N in various anaerobic codigestions of manure and lignocellulosic biomass based on artificial neural networks. Energy Fuels 2016;30(11):9490–501.
[58] Federation WE, Association APH. Standard methods for the examination of water and wastewater. Washington, DC, USA: American Public Health Association (APHA); 2005.
[59] Almomani F, Shawaqfah M, Bhosale R, Kumar A, Khraisheh M. Intermediate ozonation to enhance biogas production in batch and continuous systems using animal dung and agricultural waste. Int Biodeterior Biodegrad 2017;119:176–87.
[60] Almomani F, Bhosale RR, Kumar A. The effect of intermediate ozonation process on improving biogas production from co-digestion of agricultural waste and manure. Adv Materi – TechConnect Briefs 2016;2016(2):170–4.
[61] Koupaie EH, Leiva MB, Eskicioglu C, Dutil C. Mesophilic batch anaerobic co-digestion of fruit-juice industrial waste and municipal waste sludge: Process and cost-benefit analysis. Bioresour Technol 2014;152:66–73.
[62] Zhang C, Li J, Liu C, Liu X, Wang J, Li S, et al. Alkaline pretreatment for enhancement of biogas production from banana stem and swine manure by anaerobic codigestion. Bioresour Technol 2013;149:353–8.
[63] Almomani F, Bhosale R. Enhancing the production of biogas through anaerobic co-digestion of agricultural waste and chemical pre-treatments. Chemosphere 2020;126805.
[64] Ghatak MD, Ghatak A. Artificial neural network model to predict behavior of biogas production curve from mixed lignocellulosic co-substrates. Fuel 2018;232:178–89.
[65] Hassan M, Ding W, Shi Z, Zhao S. Methane enhancement through co-digestion of chicken manure and thermo-oxidative cleaved wheat straw with waste activated sludge: A C/N optimization case. Bioresour Technol 2016;211:534–41.
[66] Ndegwa PM, Thompson SA. Effects of C-to-N ratio on vermicomposting of biosolids. Bioresour Technol 2000;75(1):7–12.
[67] Appels L, Baeyens J, Degreve J, Dewil R. Principles and potential of the anaerobic digestion of waste-activated sludge. Prog Energy Combust Sci 2008;34(6):755–81.
[68] Joute Y, El Bari H, Belhadj S, Karouach F, Gradi Y, Stelte W, et al. Semi-continuous anaerobic co-digestion of cow manure and banana waste: effects of mixture ratio. Appl Ecol Environ Res 2016;14(2):337–49.
[69] Bollon J, Le-hyaric R, Benbelkacem H, Buffiere P. Development of a kinetic model for anaerobic dry digestion processes: Focus on acetate degradation and moisture content. Biochem Eng J 2011;56(3):212–8.
[70] Yuan H, Zhang Y, Li X, Meng Y, Liu C, Zou D, et al. Effects of Ammoniation Pretreatment at Low Moisture Content on Anaerobic Digestion Performance of Rice Straw. 2014 2014;9(4):12.
[71] Fujishima S, Miyahara T, Noike T. Effect of moisture content on anaerobic digestion of dewatered sludge: ammonia inhibition to carbohydrate removal and methane production. Water Sci Technol 2000;41(3):119–27.
[72] Angelidaki I, Ahring BK. Anaerobic thermophilic digestion of manure at different ammonia loads: Effect of temperature. Water Res 1994;28(3):727–31.
[73] Chae KJ, Jang A, Yim SK, Kim IS. The effects of digestion temperature and

temperature shock on the biogas yields from the mesophilic anaerobic digestion of swine manure. Bioresour Technol 2008;99(1):1–6.
[74] Li D, Liu S, Mi L, Li Z, Yuan Y, Yan Z, et al. Effects of feedstock ratio and organic loading rate on the anaerobic mesophilic co-digestion of rice straw and cow manure. Bioresour Technol 2015;189:319–26.
[75] Wainaina S, Lukitawesa, Kumar Awasthi M, Taherzadeh MJ. Bioengineering of anaerobic digestion for volatile fatty acids, hydrogen or methane production: A critical review. Bioengineered 2019;10(1):437–58.
[76] Yang G, Wang J. Ultrasound combined with dilute acid pretreatment of grass for improvement of fermentative hydrogen production. Bioresour Technol 2019;275:10–8.
[77] Tian M, Liu X, Li S, Liu J, Zhao Y. Biogas production characteristics of solid-state anaerobic co-digestion of banana stalks and manure. Trans Chin Soc Agric Eng 2013;29(7):177–84.
[78] Rinzema A, van Lier J, Lettinga G. Sodium inhibition of acetoclastic methanogens in granular sludge from a UASB reactor. Enzyme Microb Technol 1988;10(1):24–32.
[79] Barakat A, Monlau F, Steyer J-P, Carrere H. Effect of lignin-derived and furan compounds found in lignocellulosic hydrolysates on biomethane production. Bioresour Technol 2012;104:90–9.
[80] Bondesson P-M, Galbe M, Zacchi G. Ethanol and biogas production after steam pretreatment of corn stover with or without the addition of sulphuric acid. Biotechnol Biofuels 2013;6(1):11.
[81] Al Momani FA, Jarrah N. Treatment and kinetic study of cyanobacterial toxin by ozone. J Environ Sci Health – Part A Toxic/Hazard Substances Environ Eng 2010;45(6):719–31.
[82] Zheng M, Li X, Li L, Yang X, He Y. Enhancing anaerobic biogasification of corn stover through wet state NaOH pretreatment. Bioresour Technol 2009;100(21):5140–5.